

Compact High-Power 2-micron Transmitter for Coherent Lidar Applications

Joe Diamond, Pedro Alvarez Fernandez, and Sammy Henderson

Beyond Photonics
6205 Lookout Rd, Ste B, Boulder, CO 80301 (USA)
sammy@beyondphotonics.com

Abstract: A novel Ho:LuLF transmitter operating in an atmospheric transmission window at 2052.92 nm with significant advantages over previous transmitters is described. The transmitter utilizes a low-gain, very-compact oscillator to create long-duration pulses needed for atmospheric wind measurements followed by a very-high-gain amplifier. Both the oscillator and the amplifier are in-band pumped near 1.94 μm using a single Tm: fiber laser. The transmitter (oscillator + amplifier) produces 60 mJ 420 ns pulses at 400 Hz and has a prime power efficiency of 7.4%. The pulses are near-transform- and near-diffraction-limited and stabilize in <15 s after pump power is applied. The entire transmitter optical head, less the external fiber-coupled Tm: fiber pump laser, is very compact, and is currently being ruggedly packaged into an ~ 1.2 liter volume. This rugged and compact transmitter when coupled with an ~ 1 -meter-diameter telescope is suitable for wind measurements from space.

1. Introduction

Beyond Photonics has developed a compact high-power transmitter operating at 2052.92 nm wavelength for coherent lidar applications. The initial focus of the development is on airborne and space-based precision atmospheric wind measurement applications. The objectives in this development were to produce a compact and efficient transmitter that has a high transmitter figure of merit (TFOM) – see the Appendix for definition of the TFOM. The innovative transmitter, which we have named the *Tempest*, meets these objectives by combining four primary features.

The first feature is a very high-gain, in-band-pumped Ho:LuLF amplifier that boosts low energy 0.5 – 1 mJ input pulses to 60+ mJ at 400 Hz PRF. The high gain of this amplifier enables a very compact, low-energy oscillator to be utilized for generation of the long-duration pulses needed for precision wind or target velocity measurements.

The second feature is a low-power oscillator design that utilizes the low-gain sigma-polarized emission cross section in Ho:LuLF. This enables creation of ~ 200 ns FWHM pulse durations with ~ 1 mJ pulse energy in a very compact 35-cm-long folded cavity.

The third feature is saturation-pumping of the oscillator by transmitting the full pump power for the oscillator and amplifier through the oscillator Ho:LuLF crystal which saturates the inversion. This configuration reduces the number of independent alignment points in the transmitter and improves its waveform stability (pulse duration and energy).

The fourth feature is use of bond-in-place optics which allows the transmitter to be implemented in a very compact and rugged package by bonding many of the optical components directly to the transmitter bench. Large mounts and additional mechanical interfaces are therefore eliminated.

Each of these features is described in more detail in the following sections.

2. High Gain Amplifier

The single-pass amplifier shown schematically in Figure 1 is in-band pumped with a Tm: fiber laser operating near 1.94 μm which provides up to 100 W of CW, linearly-polarized pump power [2]. The Tm: fiber pump laser operates at a prime power efficiency of about 23% when running at high power.

To ensure good energy storage capability, low Ho doping (0.5%) is utilized in the LuLF crystals and high pump absorption is achieved by using long crystals. In our design, two

shorter crystals are used in a folded configuration. Similar high-gain amplifier designs have been implemented in the past but with significantly lower maximum energy extraction capability.[3] We designed the amplifier to operate very efficiently in a single-pass configuration since double-pass configurations lead to instabilities in the transmitter.

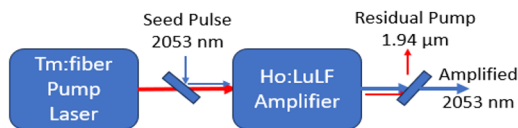


Figure 1. Amplifier functional diagram.

The amplifier output pulse energy vs incident pump power with approximately 1 mJ 400 Hz seed pulses is shown in Figure 2 for three different crystal lengths. The residual pump light is reduced, and performance increased with the longer 24 cm crystal length. This crystal length results in the 1 mJ seed pulses being amplified to 62 mJ with 61 W of incident pump power. At intermediate pump power, the optical-to-optical slope efficiency is 58%.

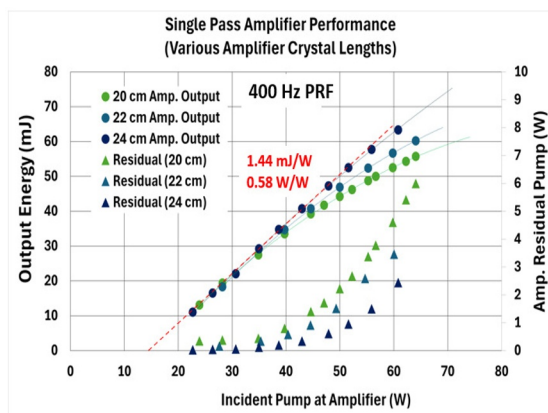


Figure 2. Amplifier output vs pump power.

The output energy vs input energy at 400 Hz PRF when the amplifier is pumped at 60 W is shown in Figure 3. The 1 mJ seed energy at 400 Hz results in efficient saturated operation of the amplifier.

Seed energies as low as 0.2 mJ can be efficiently amplified allowing the potential for low-energy, fiber-laser-based systems to be used as the amplifier seed source. Single-pass gains vary between 17 dB for 1.15 mJ seed energy and 32 dB for 25 μJ seed energy. The output of the amplifier was measured to be near diffraction limited with $M^2 \sim 1.05$.

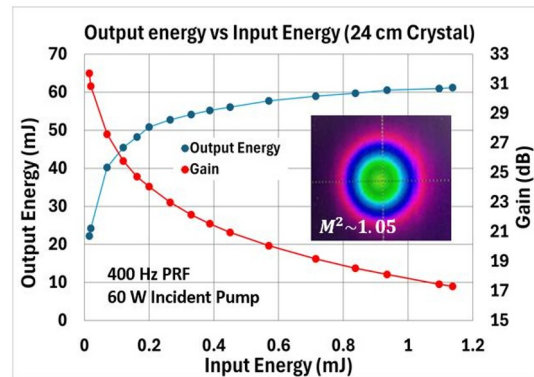


Figure 3. Amplifier output vs Seed Energy at 400 Hz PRF and 60 W incident pump power.

The amplifier output vs PRF when pumped at 60 W and seeded with ~ 1 mJ pulse energy is shown in Figure 4. At high PRFs beyond 2.5 kHz (not shown in Figure) the average output power saturates at 30 W – representing 50% optical-to-optical conversion of the 60 W incident pump power.

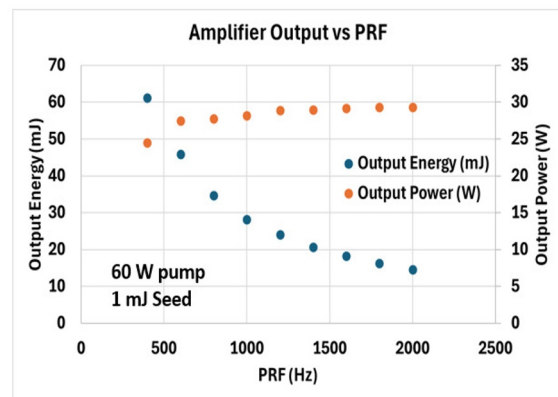


Figure 4. Amplifier output vs PRF.

We chose to nominally operate the amplifier at 400 Hz since it provides optimal TFOM with CW pumping. As shown in Figure 5, for the case of 0.5 mJ seed and 50 W pump, the *reduced* TFOM, represented by $FOM = E\sqrt{PRF}$, is near maximum at 400 Hz. The pulse width is determined by the seed pulse and is therefore not included in this reduced, amplifier-only TFOM.

Similar FOM is obtained at 300 and 350 Hz, but 400 Hz is a safer operating point from a potential optical damage perspective since the pulse energy inversely scales with PRF. At our nominal operating point of 60 mJ and 400 Hz (60 W pump and 1 mJ seed) the reduced figure of merit is $1200 \text{ mJ}\sqrt{\text{Hz}}$.

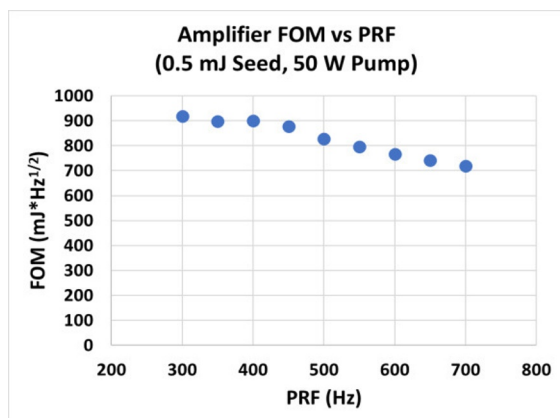


Figure 5. Amplifier FOM vs PRF for operation at 50 W pump and 0.5 mJ seed

It should be noted that due to the high gain of the amplifier, the seed pulses are pulled forward in time and stretched in duration. These effects are shown in Figure 6 where an ~ 1 mJ, 223 ns FWHM seed pulse is stretched to 422 ns FWHM while being amplified to 61.8 mJ.

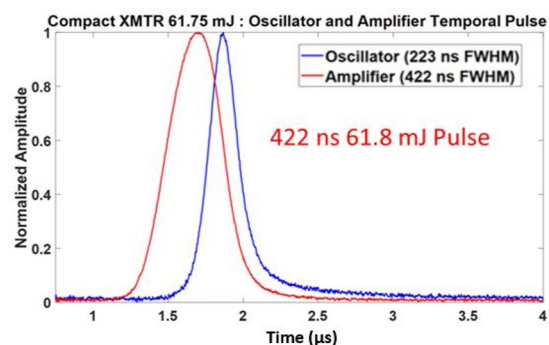


Figure 6. Amplifier pulse stretching.

Our measurements show that the amplifier has a very fast warm up time from a cold start achieving full-power, near-diffraction-limited far field patterns, and stable pointing in only 15 seconds after ramping up from a very low power simmer condition. This fast turn on characteristic makes the transmitter suitable for intermittent operation when available prime power is limited.

3. Compact Low-Power Oscillator

The efficient high-gain amplifier enables use of a very low energy oscillator for waveform generation. Long pulse durations are needed for precision wind velocity measurements and improved detection of the coherent signal in noise (see Appendix). By using the low-cross-section, sigma-polarized transition in Ho:LuLF near 2053 nm and a large mode size in the laser

crystal, we have achieved long pulse durations with ~ 1 mJ pulse energy at 400 Hz required for high-efficiency operation of the amplifier. As shown in Figure 7, the oscillator is very compact having a 35 cm long ring cavity folded into an ~ 4.2 x 2.2 inch footprint.

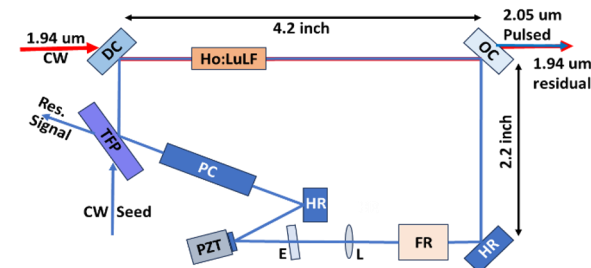


Figure 7. Compact oscillator layout.

The compact oscillator incorporates a compact Faraday rotator (FR) to maintain unidirectional operation, a lens (L) to stabilize the transverse mode, a thin etalon (E) to discriminate against the higher, sigma-polarized gain near 2065 nm, and a Q-Switch consisting of a Pockels cell (PC) and thin film polarizer (TFP). The oscillator is injection seeded through the TFP at 2052.92 nm to maintain single-frequency operation, and the intra-cavity PZT-mounted mirror is used to maintain the proper seeding condition.

The oscillator output energy and pulse duration vs the pump power absorbed in the laser crystal are shown in Figure 8.

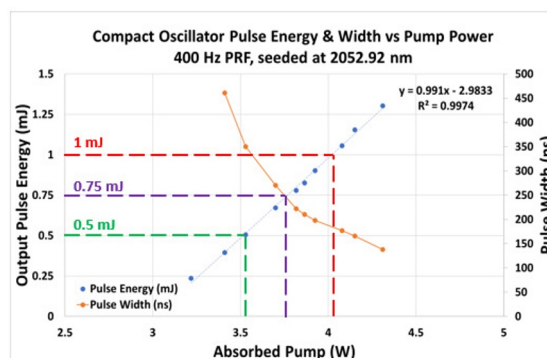


Figure 8. Compact oscillator output energy and pulse duration vs absorbed pump power.

Although the optical-to-optical efficiency of the oscillator is not very high, its power consumption represents a small portion of the total power consumed by the transmitter (oscillator + amplifier) and as such does not greatly impact the total wall plug efficiency of the transmitter.

4. Saturation Pumping of the Low-Power Oscillator

With the objective of increasing optical alignment stability by reducing the number of independent alignment points in the transmitter, we have successfully demonstrated the oscillator under saturation pumping of the laser crystal. In this configuration, all the pump power for the transmitter traverses the oscillator rod prior to being used to pump the amplifier. For pump power well above the saturation intensity in the laser crystal, the crystal becomes nearly transparent allowing a high percentage of the pump power to be transmitted to the amplifier. This configuration and the split pump configuration are illustrated in Figure 9.

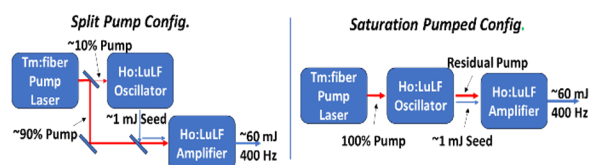


Figure 9. Split and saturation pumped configurations.

To achieve the desired pulse energy from the saturation-pumped oscillator with good efficiency, the crystal length and Ho doping concentration must be properly selected.

Saturated pumping of the oscillator results in output pulse energy and pulse duration with reduced sensitivity to pump power variations. This is shown in Figure 10 for a saturation-pumped oscillator laser crystal designed to produce 1-1.2 mJ pulse energies and 200-220 ns FWHM pulse duration.

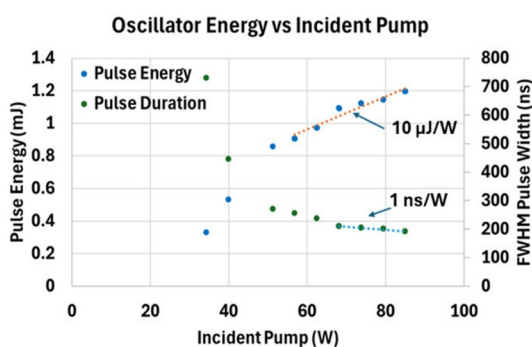


Figure 10. Saturation-pumped compact oscillator output vs incident pump power.

As illustrated in the figure, the saturation-pumped oscillator configuration has not only reduced transmitter alignment points but also

improved waveform stability (energy and pulse duration). If not well designed, the saturation pumped configuration can be less efficient than the split pump configuration due to excess absorption of the Gaussian transverse mode pump power in the oscillator crystal.

5. Compact Fabrication Approach

We have been developing a bond-in-place optics mounting approach which allows the transmitter to be implemented in a very compact and rugged package. This is achieved by bonding many of the optical components directly to the transmitter bench, therefore eliminating large mounts and additional mechanical interfaces. Optical and mechanical components are designed to be small and lightweight to endure high-vibration and shock environments. Using this approach, we are currently building the *Tempest* transmitter onto an 6 x 8 inch optical bench with the bench plus component thickness being less than 1.4 inch at the thickest point, resulting in a transmitter that is <1.2 liters in volume. This will be described further in future papers.

6. Summary

We have demonstrated a compact coherent 2-micron wavelength transmitter architecture (the *Tempest*) that represents a significant improvement over the previous generation transmitters. As shown in Table 1, the *Tempest* transmitter has significantly higher TFOM than do previous transmitters while being less than 1/10th the volume and 1/3 the mass of the earlier generation transmitters. As previously noted, the TFOM is defined in the Appendix.

The TFOM of the *Tempest* is about 2.7x and 2.0x higher than the AWP1 and AWP2 systems respectively that are described in other papers in this conference. [4,5] The 7.4% prime power efficiency of the *Tempest* transmitter is significantly higher than the efficiency of previous generation transmitters.

It should also be noted that although the *Tempest* generates substantial pulse energies, fluence levels are being properly managed and no optical damage has been experienced throughout the breadboard development. We are currently building the *Tempest* transmitter into a compact package with <1.2 liter volume. With continued development this rugged and compact transmitter when coupled with an ~ 1-

meter-diameter telescope is suitable for wind measurements from space.

Table 1. Transmitter Comparison

Parameter	DAWN	AWP 1	AWP 2	Tempest
Wavelength (nm)	2052.92	2052.92	2052.92	2052.92
Pulse Energy (mJ)	80	32	56	60
Pulse Repetition Freq. (Hz)	10	200	200	400
Average Power (W)	0.8	6.4	11.2	24
Pulse Duration, FWHM (ns)	180	360	180	420
Pulse Spectral Width (MHz)	2.5	1.2	2.5	1.3
Spectral Width Factor, K	1.0	1.0	1.0	1.2
Beam Quality, M ²	1.1	1.07	1.07	1.05
TFOM (J*rt(Hz)*ns ^{0.37})	1.56	3.72	5.04	9.97
Mechanical & Prime Power				
Oscillator Cavity Length (m)	3.6	3.6	3.6	0.35
Transmitter Volume (cm ³)	NA	11,516	11,516	1101
Transmitter Mass (kg)	12	10	10	3.35
1940 Pump Power	NA	60	70	75
QS Prime Power (W)	80	80	80	2
Pump* + QS Prime Power (W)	NA	355	388	326
Normalized TFOM wrt DAWN	1.00	2.38	3.23	6.38
Prime Power Efficiency (%)	NA	1.80%	2.89%	7.36%
		assumes using higher eff. Fibertek pump		

Acknowledgments

This work was supported under NASA SBIR, NASA ESTO, and Beyond Photonics internal funding. Other contributors to the development at Beyond Photonics were Charley Hale, Kevin Williamson, and Pat Kratovil. Support from the NASA LaRC team (Michael Kavaya, John Marketon, Kris Bedka, David MacDonnell, and Shelly Stover) has been instrumental in allowing advancement of this technology. Doruk Engin at Fibertek helped with the Tm: fiber pump laser.

Appendix: Transmitter Figure of Merit

The minimum backscatter sensitivity of a coherent lidar scales inversely with the transmitter figure of merit, so a large figure of merit is desired. The transmitter figure of merit is given by

$$TFOM = \frac{E \cdot \tau}{1 + M^2} \cdot \sqrt{\frac{PRF}{\tau}} \cdot \tau^{-\alpha} = \frac{1}{1 + M^2} \cdot E \cdot \sqrt{PRF} \cdot \tau^{0.5-\alpha},$$

where E is the pulse energy, PRF is the pulse repetition frequency, τ is the pulse FWHM duration, and M^2 is the beam quality factor (times diffraction limited far field beam divergence). For typical single-frequency pulse durations considered for coherent wind measurement lidar systems, the mean signal peak height in the spectrum is proportional to $\frac{E \cdot \tau}{1 + M^2}$. [1] The $\sqrt{PRF/\tau}$ dependence of the FOM is due to a reduction in the noise

fluctuations from averaging over multiple pulses and range resolution bins as is typically done with wind lidar systems.

The exponent, α , on the pulse duration varies with the desired probability of correct detection, P_g , of the signal peak in the spectrum of the signal plus noise when searching for the signal peak over a fixed velocity (frequency) span. Semi-analytic analysis and numerical modeling show for $P_g = 50\%$ $\alpha \approx 0.22$ and for $P_g = 90\%$ $\alpha \approx 0.13$. As P_g approaches 100%, α approaches zero. The TFOM values listed later in this paper are for $P_g = 90\%$.

It is important to note that the above TFOM equation assumes the signal spectral width is dominated by the transmitted pulse duration. When other signal spectral broadening mechanisms begin to significantly contribute, such as wind variations in the accumulated measurement volume, the sensitivity benefit of longer duration transmitter pulses (narrower transmitted spectral width) is reduced. Due to this, in many atmospheric wind measurement scenarios pulse durations > 500 ns have limited benefit in increasing the lidar sensitivity.

References

- [1] S.W. Henderson, P. Gatt, D. Rees, and R.M. Huffaker, **Wind Lidar**, book chapter in Laser Remote Sensing, Eds. Fujii and Fukuchi, CRC Press, Taylor and Francis Group, Boca Raton, FL (2005)
- [2] D. Engin, S. Litvinovitch, M. Long, H. Cao, and M. Storm, "Spaceflight 100W, 1940nm polarization maintaining Tm doped fiber laser for pumping Q-switched 2um Ho:YLF," Proc. SPIE 10899, Components and Packaging for Laser Systems V, 108990H (4 March 2019); doi: 10.1117/12.2507905
- [3] A. Dergachev, "45-dB, Compact, Single-Frequency, 2-μm Amplifier," in Lasers, Sources, and Related Photonic Devices, OSA Technical Digest (CD) (Optica Publishing Group, 2012), paper FTh4A.2.
- [4] J. Marketon, et al., "Coherent Doppler Wind Lidar Suborbital and Orbital Activities at NASA Langley," 22nd CLRC, Landshut, Germany, 23-28 June 2024
- [5] J. Marketon, K. Bedka, S. Henderson, and M. Kavaya, "NASA's Aerosol Wind Profiler," 22nd CLRC, Landshut, Germany, 23-28 June 2024.